JOURNAL OF SOLID STATE CHEMISTRY **121,** 111–116 (1996)
ARTICLE NO. 0016

Lattice-Energy Conformational Analysis of Orthosilicate Ca_3OSiO_4 (C_3S): Regularizing Ca-Sublattice versus Deforming SiO_4^{4-} Anions

Jose Fayos

Departamento de Cristalografia, Instituto Rocasolano, Serrano 119, Madrid 28006, Spain

and

Mercedes Perez-Mendez

Instituto de Ciencia y Tecnologia de Polimeros, Juan de la Cierva 3, Madrid 28006, Spain

Received February 13, 1995; in revised form August 15, 1995: accepted August 21, 1995

Orthosilicate Ca_3OSiO_4, and other related compounds, preserves the fcc or hcp structure of metallic Ca, where some Ca are substituted by SiO_4 and the oxygens fill the octahedral holes. The SiO_4^{4-} anions deform the cubooctahedral cage Ca_{12} around them, and this deformation propagates along the crystal. Both the preferred orientations of SiO_4 and the induced deformations of the Ca sublattice, which were previously observed by XRD, are now predicted by simple lattice-energy conformational analysis, where the match is improved when the potential model includes weak Ca–Ca covalent bonds between neighboring cations. The polytypism of Ca_3OSiO_4 is explained by the presence of different arrangements of the SiO_4 orientations in the crystal. The transition between polytypes with the temperature being of the order–disorder type. © 1996 Academic Press, Inc.

1. INTRODUCTION

Crystallochemistry of silicates has been drawing attention for a long time, resulting in the general survey (1) or the more specific study of orthosilicates (2). The orthosilicate Ca_3OSiO_4 is the principal component (C_3S) of Portland cement which, with decreasing synthesis temperature, presents three polytypes, rhombohedral, monoclinic, and triclinic. A previous crystallochemical review (3) on these crystal structures and other six related phases, all with formula M_3OXO_4 (M = Ca, Sr, Ba, Cd, Pb and X = Si, Ge) showed that they can be classified into three idealized structural models (the three polytypes of C_3S belong to the same model). All these compounds, like CaO, preserve the close-packed (fcc or hcp) structure of metallic Ca. In CaO the oxygens fill the metallic octahedral holes, forming a NaCl-type structure, where the Ca–Ca distance, in the metallic sublattice, is reduced from 3.94 Å in fcc Ca to 3.39 Å in the oxide. In the Ca_3OSiO_4-like models, a quarter of the Ca atoms are substituted by SiO_4, whereas the free oxygens fill the octahedral holes. In this case, the Ca–Ca distance in the sublattice is reduced to 3.54 Å.

The use of the metallic sublattice to describe a crystal structure has been well established for many inorganic compounds (4). We have two metallic polyhedra in our orthosilicates, the octahedral (OCT) Ca_6 cages surrounding the free oxygens and the cubooctahedral (CUB) Ca_{12} cages, shown in Figs. 1 and 2, including SiO_4. The three structural models for M_3OXO_4, mentioned in the previous paragraph, correspond either to different arrangements of the included SiO_4 in the metallic lattice or to different ways of packing the Ca_6 and Ca_{12} cages. Their space groups are $R\bar{3}m$ or $P6_3mc$, with the common subgroup $P3m1$, where the anions SiO_4 are on the threefold axes. These models are, in fact, those packings producing the shortest c-axes in the unit cell. It is noteworthy that the observed size of the Ca_{12} cage is independent of the size of the included XO_4 group (Si–O = 1.62 Å or Ge–O = 1.77 Å), which suggests some stability for the metallic sublattice.

The fact that the metallic structure is preserved in the derived compounds, which is also reported in many other compounds (5, 6), adds a more chemical meaning to the merely descriptive function of the metallic sublattice. In fact, we will include a weak strength for this sublattice to model a convenient lattice-energy potential.

The observed crystal structures of the Ca_3OSiO_4-like compounds present two common features (3): (a) The orientation of the SiO_4 group is one of the two shown in Fig. 2, or both in statistical disorder, which suggests that SiO_4 has some freedom to rotate into its Ca_{12} cage. (b) There

0022-4596/96 $12.00

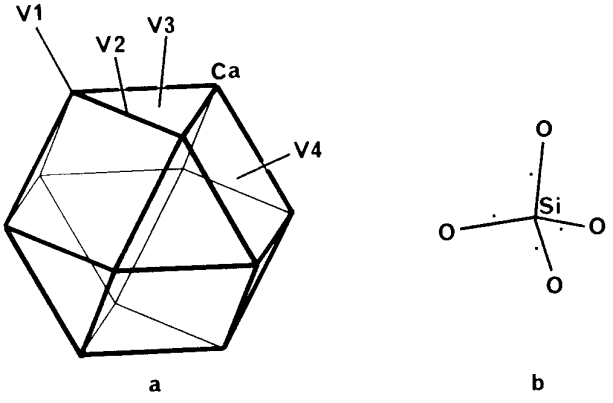

FIG. 1. (a) A Ca_{12} (CUBC) unit showing its more symmetrical directions, and (b) The SiO_4^{4-} group, where the four electrons of the anion charge are represented by points attached to the Si–O single bonds.

is a contraction of the metallic lattice along the *c*-axes which causes two different Ca–Ca distances, i.e., those perpendicular to the *c*-axis (or to V3 in Fig. 1a) with $d_\perp = 3.575$ Å, and the rest of the distances with $d_\parallel = 3.511$ Å; which suggests that SiO_4 deforms its Ca_{12} cage, communicating its own $3m$ symmetry to the whole lattice (P3m1).

In this work, we have calculated the more stable orientations of SiO_4 into the Ca_{12} cage, the corresponding cage deformations induced by those orientations and, hence, the deformation of the metallic sublattice. A simple lattice-energy conformational analysis was used, where the potential maps were calculated for some selected packing variables.

2. THE VAN DER WAALS LATTICE POTENTIAL MODEL

Since orthosilicates are typical ionic crystals, and in order to avoid the use of undetermined potential parameters, we began with the simplest Van der Waals (VDW) potential form,

$$U(\mathrm{VDW}) = \sum (Kq_iq_j/r_{ij} + A_{ij}/r_{ij}^{12}), \qquad [1]$$

that is, a Coulombian field between point charge atoms plus a repulsive term to prevent atomic collisions.

We began the analysis by considering only the intra-r_{ij} in isolated Ca_6O and $Ca_{12}SiO_4$ groups, which, although being a drastic simplification, gave good results as shown latter.

The atomic charges q_i were estimated assuming the charge distribution $Ca_3^{2+}O^{2-}(SiO_4)^{4-}$. The charge of Ca in the crystal lattice is $+2\,e$, however if we are only interested in the internal interactions of the isolated CUB and OCT, such charges would exploit the Ca cages. Hence, for calculations on isolated polyhedra, as one Ca belongs to 4 CUB and 2 OCT, we assumed that each Ca interacts with a single polyhedron, as it would have the charge $+2/6e = +1/3\,e$. Then, both Ca_6O or $Ca_{12}(SiO_4)$ have a total charge of zero.

The net charge of $-4\,e$ for SiO_4 should be distributed into the group. However, we were not interested in the Si charge, as we did not consider any Si–OC or Si–Ca atomic interactions, first because we assumed rigid SiO_4, so its internal contribution to U(VDW) becomes constant, and second, to avoid the reported screening effect of the four oxygens between Si and Ca (7). We had to evaluate, however, the charge of the four oxygens of SiO_4, which we will call OC to distinguish them from the free O included in OCT with charge $-2\,e$. We assumed that some of the four electrons of the anion are on the short Si–OC bonds (see Fig. 1b), while the rest of the anionic charge is attached to the four OCs. As a source, we had the oxygen charge in two compounds, where the Si–O bond lengths are of 1.62 Å, like in our SiO_4 group. The experimental value of $q(\mathrm{O}) = -0.61\,e$, found in the deformation difference electron density map of quartz SiO_2 (8), and the close value of $q(\mathrm{O}) = -0.81\,e$, calculated for the nonbridging O atoms of α-Mg_2SiO_4, by semi-empirical molecular-orbital (CNDO/2) (9). For our SiO_4 group, we considered two alternative hypotheses for the charge of OC. In the first, we assumed that $\frac{1}{2}\,e$ is attached to each OC, or $q(\mathrm{OC}) = -0.5\,e$. In a second hypothesis we considered the different electronegativities of Si (1.8) and O (3.5) (10), which moves the charge toward OC, giving a more realistic value of $q(\mathrm{OC}) = -0.75\,e$.

Regarding the values of K and A_{ij} in Eq. [1], we took the dielectric constant of vacuum, which corresponds to $K = 332.4$ Kcal mol^{-1} Å e^{-2}, and different repulsion parameters for each pair of atomic species. The A_{ij} repulsive parameters, were calculated assuming that at the equilibrium interatomic distance (r_0), $(\partial U/\partial r)_{r=r_0} = 0$, which applied to Eq. [1] gives $A_{ij} = |Kr_{\mathrm{O},ij}{}^{11}q_iq_j/12|$. We took for $r_{\mathrm{O},ij}$ the sum of the ionic radii (R_i) of the atomic pair, where $R_{\mathrm{Ca}} \simeq 1.0$ Å and $R_{\mathrm{O}} \simeq 1.4$ Å (11). Considering the charges

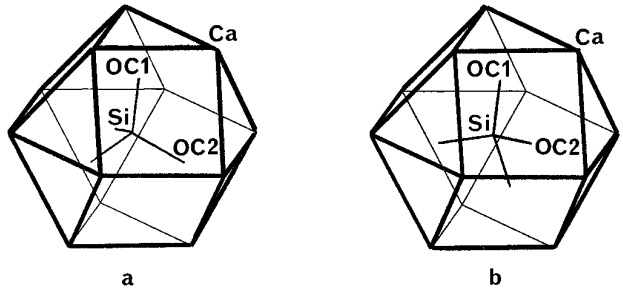

FIG. 2. Ca_{12} cubooctahedra (CUBH) showing the two preferred orientations, V33 (a) and V34 (b), of SiO_4. Si–OC1 is the rotation axis of SiO_4 during the conformational analysis.

q(OC) = −0.5 or q(OC) = −0.75, q(O) = −2 e and q(Ca) = +1/3 e for isolated polyhedra, we got the following values of A_{ij} (in Kcal mol^{-1} Å^{12}): A[Ca, Ca] = 6296, A[Ca, OC(0.5 e)] = 70166, A[Ca, OC(0.75 e)] = 105250, A[Ca, O] = 280666, A[OC(0.5 e), OC(0.5 e)] = 573634, A[OC(0.75 e), OC(0.75 e)] = 1290677, A(OC(0.5 e), O] = 2294538, A[OC(0.75 e), O] = 3441806, and A[O, O] = 9178150.

A full minimization of U(VDW) in Eq. [1] for isolated polyhedra would imply 21 atomic interactions for the Ca_6O octahedron and 136 for the $Ca_{12}SiO_4$ cuboctahedron. Instead, we decided to approach this search by the conformational analysis of Eq. [1], in the space of a few geometrical variables. These variables, which define the structure of the isolated polyhedra, were selected in accordance with the idealized models described above, that is the orientation of SiO_4 and the flattening of the CUB and OCT cages. The optimal structures producing U-minima, were sought by mapping U versus those variables.

We found the best geometry of the isolated groups by relaxing the free variables, step by step. The following steps were used:

(I) The Ca_{12} cubooctahedron, which has been observed as cubic (CUBC) (Fig. 1a) or hexagonal (CUBH) (Fig. 2), is assumed to be regular with the observed average Ca–Ca distance of 3.543 Å. The SiO_4, in the center of the CUB, is a rigid regular tetrahedron (Fig. 1b) with the observed bond distance Si–O = 1.625 Å. The variables in U(VDW) are the orientation of a bond Si–OC1, which we take as the SiO_4 rotation axis, and the rotation of SiO_4 about this axis.

(II) The CUB and OCT polyhedra, the latter with the oxygen in the center, remain regular, but their size or the Ca–Ca distance is a new variable, together with the orientation of SiO_4.

(III) Deformation of CUB and OCT are allowed along one of their threefold axes (that parallel to Si–OC1), and the two Ca–Ca variables $d_\perp$ and $d_\parallel$ are now added to those of the SiO_4 orientation.

Finally, we used the geometries of CUB and OCT units, which have been optmized above, to calculate the geometry of the whole crystal lattice.

3. RESULTS

3.1. Conformational Analysis Applied to Isolated Polyhedra and Extended to the Lattice

By applying step I for a total free orientation of SiO_4 in a CUBC, we found that potential minima appeared when the bond Si–OC1 was oriented along any internal symmetry element of the Ca_{12} cage. Hence, a finer step I was repeated, where Si–OC1 was successively oriented toward a square face (V4), a triangular face (V3), a Ca–Ca edge (V2), and toward one Ca (V1) (see the Fig. 1a), with SiO_4 being rotated within 120° about Si–OC1, for each orientation. The later rotation is defined by the orientation of any Si–OC2 bond, as it is shown in Fig. 2. The best SiO_4 orientations were V33 where the four Si–OC are oriented along V3 directions and V34 where Si–OC1 is oriented along V3 and the three Si-OC2 are as close as possible to V4, which is obtained by a 60° rotation of V33 around Si–OC1. The first line in Table 1 shows the U-minima for a CUBC of edge 3.543 Å with charges q(Ca) = +1/3 and q(OC) = −1/2, where the optimal rotations of SiO_4 are only indicated for the lowest minima, that is, V33 and V34.

Next, step II was applied to find the best Ca–Ca distances of the regular CUBC and the best SiO_4 orientations. Table 1 shows both variables together with the correspondent U-minima. Step II was also applied to an OCT Ca_6O, which gave a potential minimum of −356 Kcal mol^{-1} for an edge Ca–Ca = 3.49 Å. We noted that this edge was shorter than those calculated for a CUBC, although they should be equal because OCT and CUBC share faces in the crystal.

By considering q(OC) = −0.75 e, steps I and II, when applied to a CUBC, gave the same relative U-minima as shown in Table 1 for q(OC) = −0.5 e, although with different values. On the other hand, steps I and II applied to a CUBH gave resuls very close to that found for CUBC. Some of the above results are shown in the first two lines of Table 2. Hence, in any case, Table 1 is representative of (a) the best SiO_4 orientations in a Ca_{12} cage, (b) the best size of the cages, and (c) the respective U-minima, both for CUBC or CUBH and also for q(OC) = −0.5 or −0.75 e.

At this point, we realized that the optimal Ca–Ca distances, for the preferred orientations V33 and V34, were the closest to the observed average value of 3.54 Å, among the Ca_3OSiO_4-like compounds. And we also noted that the best (V3) orientation of Si–OC1, coincided with the c-cell direction where the flattening is observed in the crystals. Hence, we decided to fix this V3 orientation of SiO_4 for the next calculations.

Step III applied to a CUBC or a CUBH produced a significant Ca_{12} flattening for the V34 orientation, yielding to $d_\perp$ = 3.70 Å and $d_\parallel$ = 3.37 Å for q(OC) = −0.5, and to $d_\perp$ = 3.65 Å and $d_\parallel$ = 3.11 Å for q(OC) = −0.75. For the V33 orientation, however, step III produced regular Ca_{12}, or $d_\parallel = d_\perp$, which is probable due to the coincidence of the threefold axes of both SiO_4 and Ca_{12} groups.

The next step would be to compare these optimal geometries calculated by our conformational analysis, on isolated polyhedra, with the observed geometry in the real crystals. For that, we approached the geometry of the whole Ca sublattice from the optimized Ca_6 and Ca_{12} cages as follows. Considering that every Ca–Ca edge belongs to two CUB and one OCT, we assumed that the potential of the crystal

TABLE 1
Conformational Analysis of Isolated $Ca_{12}SiO_4$ (CUBC) Groups

SiO_4 orientation	V4	V33	V34	V2	V1	Step
U(VDW) for Ca–Ca = 3.543 Å	−211	−217	−218	−215	−195	I
Minima U(VDW) for the optimal Ca–Ca (Å)	−214	−219	−219	−217	−210	II
	3.70	3.63	3.59	3.65	3.78	

Note. In the first line are the VDW potentials, in Kcal mol^{-1}, for different Si–OC1 orientations of SiO_4 into is Ca_{12} cage (step I). In the second line are the U-minima for the optimized Ca–Ca length in regular Ca_{12} (step II). The used charges are $q(Ca) = +1/3\ e$ and $q(OC) = -0.5\ e$.

is $U(CR) \sim 2U(CUB) + U(OCT)$. Then the shorter Ca–Ca distances in the crystal lattice would be given by

$$d_i(CR) = [2U(CUB)/U(CR)]d_i(CUB) + [U(OCT)/U(CR)]d(OCT), \quad [2]$$

where $d_i(CUB)$ and $d(OCT)$ apply to the Ca–Ca edges in the isolated polyhedra, while $d_i(CR)$ are the Ca–Ca distances in the crystal, which could be unique for regular polyhedra, or have two values $d_\perp(CR)$ and $d_\parallel(CR)$ for a flattened crystal. In fact, there are compounds (3) where the SiO_4 has the two preferred orientations V34 and V33 in them, while the flattened V34 CUBs would contribute to flatten the lattice; the regular OCT's and V33 CUBs would regularize it.

Equation [2] applied to the optimized CUB and OCT gave, for $q(OC) = -0.5\ e$, a regular crystal V33 with $d(CR) = 3.57$ Å or a flattened crystal V34 with $d_\perp(CR) = 3.60$ and $d_\parallel(CR) = 3.43$ Å, while for $q(OC) = -0.75\ e$ we had $d(CR) = 3.51$ Å for V33 or $d_\perp(CR) = 3.61$ Å and $d_\parallel(CR) = 3.20$ Å for V34 orientations. Although these results are closer to the observed structures than those corresponding to isolated cages, they still deviate from the observed average values $d_\perp \simeq 3.575$ Å and $d_\parallel \simeq 3.511$ Å. The observed flattening, $d_\perp/d_\parallel$, is lower than those calculated and, besides, $d_\parallel^{cal} - d_\parallel^{obs} > d_\perp^{cal} - d_\perp^{obs}$. Both discrepancies seem to be inherent to the potential that was used, so that they would not be eliminated by a reasonable change of the charges or A_{ij} in Eq. [1]. Although the total crystal flattening depends on the population rate of the orientations (V34/V33) included in Eq. [2], there was no way to match the calculated and observed flattening by an appropriate V34/V33 ratio. Hence, in order to improve the fit, we had to modify the potential model of Eq. [1], which will be explained in Section 3.3.

3.2. Conformational Analysis Applied to a Crystal Fragment

Before modifying the potential, the reliability of Eq. [2] for building the Ca sublattice from isolated Ca cages was tested. We did it by calculating, through Eq. [1], the potential U(VDW) in a big crystal fragment from one of the structural models proposed for Ca_3OSiO_4 (3), the antiperovskite-type, with 3CUBC + 3OCT in the unit cell of dimensions $a = b = 7.15$ Å and $c = 8.52$ Å and space group $R\bar{3}m$. A fragment of size $3a \times 3b \times 3c = 27$ cells was generated which includes $Ca_{243}O_{81}Si_{81}(OC)_{324}$, where we took the charges $q(Ca) = +2\ e$, $q(O) = -2\ e$, and $q(OC) = -\frac{1}{2}\ e$. The potential U(VDW) was calculated for all r_{ij} interactions between the atoms of one CUB and one OCT, in the center of the crystal fragment, and the rest of the atoms in the fragment. The maximum interaction distance was of $\simeq 12$ Å, from which the potential almost converged. We took as variables of U(VDW) the two Ca–Ca distances $d_\perp$ and $d_\parallel$. For each pair of values we generated the whole crystal fragment, and the corresponding U(VDW) was calculated. In this way, two $U(VDW) = f(d_\perp, d_\parallel)$ maps were drawn, one assuming the V34 orientation of SiO_4 among the 81 Ca_{12} cages and the other assuming the V33 orientation for all cages. Both maps were similar, showing badly defined minima in a 0.2 Å broad area, nevertheless, the center of this area at ($d_\perp = 3.60$, $d_\parallel = 3.45$) was close to the optimal crystal geometry calculated by Eqs. [1] and [2]. Then, although the crystal fragment analysis did not give the optimized lattice geometry, with sufficient resolution, it was useful enough to support the reliability of Eq. [2].

3.3. Introduction of a Molecular Mechanics Term into the Lattice Potential

As mentioned in the last paragraph of Section 3.1, we tried to correct the calculated crystal flattening to the observed one by modifying the potential model of Eq. [1], in the sense of introducing some strength in the Ca polyhedra, which in fact is consistent with the assumed stability of the metallic sublattice. Still considering isolated polyhedra, a molecular mechanic (MME) stretching term, or some degree of covalency between close Ca's, was added to Eq. [1]. We used the term $U(MME) = \frac{1}{2}K_b \Sigma (d_i - d_O)^2$, where

TABLE 2

The Lattice-Conformational Analysis of U(VDW) (lines 1–3), and U(TOTAL) = U(VDW) + U(MME) Potentials for Isolated Ca_{12} (SiO_4) (CUBC or CUBH), with the Different Orientations V34 and V33 of the SiO_4^{4-} Anion, and for Isolated Ca_6O (OCT) Groups

Conditions	CUBC-V34	CUBH-V34	CUBC-V33	CUBH-V33	OCT
U (VDW) (min)	−582.79	−581.49	−578.84	−580.03	−356.31
d	3.470	3.471	3.517	3.517	3.496
d (CR)	(3.475)	(3.475)	(3.512)	(3.512)	
$1/2K_b$ for d_O (Cr)	2.4	2.4	1.0	1.0	1.6
U (TOTAL)	−571.88	−570.79	−575.00	−576.43	−352.99
U (TOTAL)	−574.59	−572.92			
$d_\perp$, $d_\parallel$	3.64 3.35	3.63 3.35			
$d_\perp$ (CR), $d_\parallel$ (CR)	(3.62 3.39)	(3.61 3.39)			

Note. The charges used are q(Ca) = +1/3 e q(OC) = −0.75 e, and q(O) = −2 e. The optimal Ca–Ca distances (Å), which minimizes U (Kcal mol^{-1}), are d, for regular, or $d_\perp$ and $d_\parallel$, for flattened polyhedra. In parenthesis are the corrected distances for a crystal. The partial force constants K_b (Kcal mol^{-1}Å^{-2}), are calculated for isolated polyhedra.

d_i are the variable distances between neighboring Ca's ($d_\perp$ or $d_\parallel$ in our model), d_O is their equilibrium distance, and K_b is the stretching force constant for the Ca–Ca bond. If we consider the metallic sublattice in the compound as a contraction of the original metallic lattice by the Coulombic forces, d_O should be 3.94 Å, which is the Ca–Ca distance in metallic Ca, and K_b should allow the contraction to the observed d_O(CR) = 3.543 Å. This means that, in the absence of such lattice strength, the VDW-optimal d(CR) should be lower than the observed D_O(CR), which occurs for q(OC) = −0.75 e, where d(CR) < 3.51 Å, but not for q(OC) = −0.5 e, where d(CR) > 3.55 Å. Thus, we assumed the more reasonable hypothesis, q(OC) = −0.75 e, to proceed with the new potential model. Before adding the MME term, Table 2 shows the U(VDW)-minima for the optimized Ca–Ca edges, both for regular polyhedra and lattices, assuming q(OC) = −0.75 e. Then, we introduced the MME term and first calculated the optimal partial-K_b of the Ca–Ca edges, referred to isolated regular OCT and CUB, by $[\partial U(\text{TOTAL})/\partial d]_{d=d_O(\text{CR})} = 0$, where U(TOTAL) = U(VDW) + U(MME). The best values for $\frac{1}{2}K_b$ and the U(TOTAL)-minima are shown in Table 2, where the small K_b are consistent with the assumed big contraction of the Ca sublattice from Ca–Ca = 3.94 Å to Ca–Ca = 3.54 Å. Note that the partial K_b of Table 2 refer to one isolated polyhedra; hence, as a Ca–Ca bond belongs to one OCT and two CUB, the total force constant of a Ca–Ca bond in the crystal would be the sum of the three partial values from the contributing polyhedra.

Next, lattice-conformational analysis of U(TOTAL) versus $d_\perp$ and $d_\parallel$ were done for the two optimal SiO_4 orientations and, as expected, the OCT and CUB with the SiO_4 in V33 orientation remained regular, while the CUB with the SiO_4 in V34 orientation were flattened. Hence, at the bottom of Table 2, we only show the U(TOTAL)-minima and flattening of the isolated polyhedra and crystal for the V34 orientation of SiO_4. This crystal flattening, where the V34 orientation is assumed in all CUB of the crystal, is still greater than the observed values of 3.575 and 3.511 Å; nevertheless, both adjust for a V34/V33 ratio of 0.47, giving $d_\perp$ = 3.567 Å and $d_\parallel$ = 3.495 Å. This solution would correspond to the statistical disorder of SiO_4 observed in some structures.

Finally, the conformational analysis gave more significant data, on the gradients of U(TOTAL), where $|\partial U/\partial d_i|$ is lower in the negative slope of U and $\partial U/\partial d_\perp > \partial U/\partial d_\parallel$, and on the potential barriers between U(V34-CUB) and U(V33-CUB), which were $\simeq$ 3.5 Kcal mol^{-1}.

4. THE POLYTYPISM OF Ca_3OSiO_4

For a given $Ca_{12}SiO_4$ CUB, there could be two V33 and eight V34 SiO_4 orientations but, as CUBs and OCTs are joining faces in the crystal, some of the neighboring SiO_4 orientations could produce OC..OC distances that are too short. Actually, the only forbidden situation is when two mutually centrosymmetric V34 orientations have OCs pointing towards a shared square CUB face, which gives the forbidden OC..OC distance of 2.0 Å. Any other mutual orientation of two SiO_4 is geometrically allowed.

We suggest that the different polytypes of Ca_3OSiO_4, which include CUBC and CUBH polyhedra, are produced by different arrangements of the orientation of neighboring SiO_4. Besides, if we consider the low potential barriers between the different SiO_4 orientations, there could be an order–disorder phase transition between these polytypes, with the temperature. On the other hand, the presence of large periodicities in the locally random-oriented SiO_4

would account for the crystal superlattices observed by electron diffraction in these polytypes (12).

5. CONCLUSIONS

A lattice-energy conformational analysis was done for Ca_3OSiO_4-like structures, where a simple potential model was used, involving a minimum number of potential parameters. The geometrical variables of the conformational maps were those which define the geometry of the idealized structures. The analysis was reliable enough to predict the observed structural geometry. The results suggest that, while the fcc or hcp Ca sublattice regularizes the crystal, the SiO_4 groups communicate their lower symmetry, flattening that sublattice along a threefold axis. This flattening corresponds to an optimal SiO_4 orientation into the Ca_{12} cage. Both the lattice flattening and the SiO_4 orientation agree with the crystal structures observed by X-ray diffraction.

In the analysis, we first used the simplest potential for ionic crystals, which predicted the optimal orientations of SiO_4; however, in order to match the calculated Ca–Ca distances with the observed ones, we considered the weak covalent bond character between neighboring Ca cations. This assumption was originated by taking into account the stability of the metallic sublattices, observed in these and other compounds. The calculated force constant of these Ca–Ca "bonds" is $\simeq$10 Kcal mol^{-1} Å^{-2}, which is only $\simeq$1/60 of the force constant assumed for the Csp^3–Csp^3 bond. However, this difference is comparable to that between the moduli of normal elasticity, which is 20 GN m^{-2} for annealed Ca versus 1050 GN m^{-2} for diamond (13). In addition, that small Ca–Ca strength is consistent with the assumed large contraction of the Ca–Ca bond length in the compound (Ca–Ca = 3.54 Å) from the metal value at the equilibrium distance Ca–Ca = 3.94 Å.

Finally, it is suggested that the observed polytypism of Ca_3OSiO_4, due to the different deformation of the metallic sublattice, is induced by different arrangements of the two preferred SiO_4 orientations in the crystal, and the three polytypes would interchange by order–disorder phase transitions with the temperature. We suggest that the superlattices observed by ED in these polytypes, could be due to a long-range periodicity of the local orientational disorder.

REFERENCES

1. F. Liebau, "Structural Chemistry of Silicates." Springer-Verlag, Berlin, 1985.
2. W. Eysel and K.-H. Breuer, *Z. Kristallogr.* **163,** 1 (1983).
3. J. Fayos and M. Perez-Mendez, *Am. Ceram. Soc. Bull.* **65**(8), 1191 (1986).
4. M. O'Keeffe and B. G. Hyde, *Struct. Bonding* **61,** 77 (1985).
5. A. Vegas, A. Romero, and M. Martinez-Ripoll, *J. Solid State Chem.* **88,** 594 (1990).
6. A. Vegas, A. Romero, and M. Martinez-Ripoll, *Acta Crystallogr.* **B47,** 17 (1991).
7. M. Matsui and T. Matsumoto, *Acta Crystallogr.* **A38,** 513 (1982).
8. N. Thong and D. Schwarzenbach, *Acta Crystallogr.* **A35,** 658 (1979).
9. T. J. McLarnan, R. J. Hill, and G. V. Gibbs, *Aust. J. Chem.* **32,** 949 (1979).
10. R. Skorczyk, *Acta Crystallogr.* **A32,** 447 (1976).
11. B. K. Vainstein, V. M. Fridkin, and V. L. Indenbom, "Modern Crystallography II," Springer Series in Solid-State Sciences 21, pp. 78–80. Springer-Verlag, Berlin, 1982.
12. M. Perez-Mendez, G. W. Groves, and J. Fayos, *J. Am. Ceram. Soc.* **69**(9), 670 (1986).
13. G. V. Samsonov, "Handbook of the Physicochemical Properties of the Elements," p. 388. IFI/Plenum, New York, 1968.